JOC Articles

Anion and Carboxylic Acid Binding to Monotopic and Ditopic Amidopyridine Macrocycles

Ivan V. Korendovych,[†] Mimi Cho,[†] Olga V. Makhlynets,[†] Phillip L. Butler,[†] Richard J. Staples,[‡] and Elena V. Rybak-Akimova*[,†]

Department of Chemistry, Tufts University, 62 Talbot Avenue, Medford, Massachusetts 02155, and Department of Chemistry and Chemical Biology, Harvard University, 12 Oxford Street, Cambridge, Massachusetts 02138

elena.rybak-akimova@tufts.edu

Received January 18, 2008

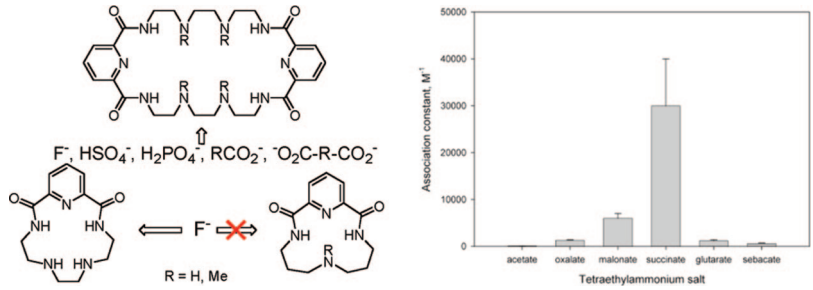

Binding of inorganic anions, carboxylic acids, and tetraalkylammonium carboxylates by macrocyclic compounds of different size was studied by NMR in DMSO-d_6. It has been shown that at least a 15-membered ring is necessary for successful recognition of fluoride. Larger macrocycles were shown to bind HSO_4^-, $H_2PO_4^-$, Cl^-, and carboxylic acid salts. Effects of binding topicity are discussed. The 30-membered macrocycles **4** and **4m** selectively bind substrates that are size- and shape-complementary: maximum binding is observed for dicarboxylic acids and dicarboxylates with four-carbon chains, and the binding constant for association of fumaric acid and **4** is ca. 5 orders of magnitude higher than that of maleic acid. The 30-membered macrocycle **4m** showed selectivity toward α-ketocarboxylic acids. Secondary amino groups were not crucial for binding of fluoride to the macrocycles; however, they proved to be very important for selectivity and strength of carboxylic acid binding. The X-ray structure of the adduct of **4** and nitrobenzoic acid confirmed the guest H-bonding with both the amide and the secondary amino groups of the 30-membered macrocyclic host.

Introduction

Recognition of inorganic and organic acids as well as their corresponding anions is a rapidly expanding area of interest. These types of guests are essential for the activity of enzymes, transport of hormones, protein synthesis, and DNA regulation.[1] Dicarboxylic acids and their anions remain among the most attractive targets for molecular recognition[1–9] since the presence of several carboxylate functional groups is typical for a variety of biomolecules, ranging from simple aliphatic di- and tricar-

* Corresponding author. Fax: 617-627-3443.
[†] Tufts University.
[‡] Harvard University.

(1) Bianchi, A.; Bowman-James, K.; Garcia-Espana, E. *Supramolecular Chemistry of Anions*; Wiley-VCH: New York, 1997.
(2) Lehn, J.-M. *Supramolecular Chemistry: Concepts and Perspectives*; Wiley-VCH: New York, 1995.
(3) Ragusa, A.; Rossi, S.; Hayes, J. M.; Stein, M.; Kilburn, J. D. *Chem. Eur. J.* **2005**, *11*, 5674–5688.
(4) Fitzmaurice, R. J.; Kyne, G. M.; Douheret, D.; Kilburn, J. D. *J. Chem. Soc., Perkin Trans. 1* **2002**, *841*, 864.
(5) Disch, J. S.; Staples, R. J.; Concolino, T. E.; Haas, T. E.; Rybak-Akimova, E. V. *Inorg. Chem.* **2003**, *42*, 6749–6763.
(6) Korendovych, I. V.; Cho, M.; Butler, P. L.; Staples, R. J.; Rybak-Akimova, E. V. *Org. Lett.* **2006**, *8*, 3171–3174.
(7) Rybak-Akimova, E. V. *Rev. Inorg. Chem.* **2001**, *21*, 207–298.
(8) Kryatova, O. P.; Kolchinski, A. G.; Rybak-Akimova, E. V. *J. Incl. Phenom. Macrocycl. Chem.* **2002**, *42*, 251–260.

10.1021/jo800128r CCC: $40.75
Published on Web 04/09/2008

SCHEME 1. Synthesis of 1, 2a, 2b, 4, and 4m

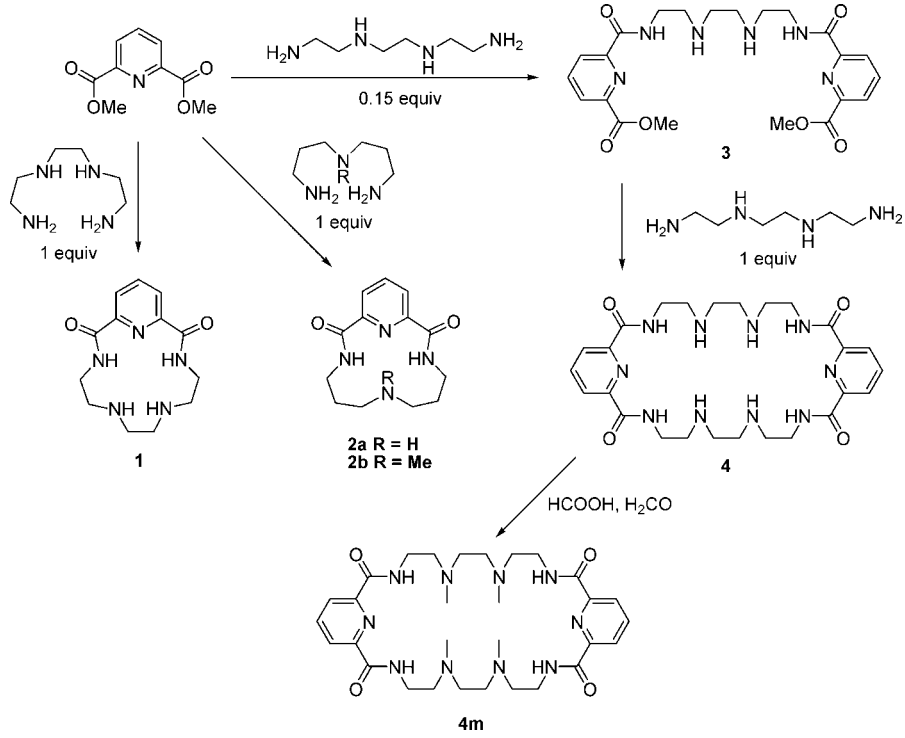

boxylic acids involved in the citric acid cycle to amino acids and proteins.

Progress in this area has led to the design of strong and selective receptors for anion binding.[1,10–12] However, full understanding of principles that govern anion recognition has not been achieved. It became clear early on that multiple hydrogen-bonding interactions are necessary for the design of high-affinity anion binding sites.[1,2] Charge and shape complementarity between the host and the anionic guests are also important. The overall ligand topology (e.g., macrocyclic or macrobicyclic) has a profound influence on anion binding, so the majority of efficient anion binding receptors are based on macrocyclic structures.[12–14]

Previous systematic studies identified the importance of ring size for anion binding affinity.[12,15–17] As the size of the macrocyclic ring gradually increases, certain large macrocyclic hosts became capable of binding more than one molecule of guest.[18,19] Despite these interesting findings, questions remain about the topicity of anion binding in solution, especially in the case of larger rings.

Progress in the field also has led to the development of several well-established motifs for anion recognition: isophthalic,[20] 2,6-bis(carbamoyl)pyridine,[21] 2,5-diamidopyrrole,[22] guanidinium derivatives,[23] and substituted ureas.[24] Combining several different binding motifs proved to be beneficial for both sensitivity and selectivity for different carboxylates.[3,4] However, the challenge of designing efficient anion and small molecule binding hosts by creating an ensemble of several binding motifs to enhance the interaction remains unmet. Earlier we have prepared a family of receptors for dicarboxylic acids based on a nickel(II) cyclidene platform with two cyclic tetraamine (cyclen) or two aminopyridine binding cites, which displayed notable length- and shape-selectivity.[5,8]

In this paper, we are addressing the questions of topicity and affinity of anion binding by introducing large, yet controllable changes in the macrocyclic hosts, and comparing small monomeric and corresponding large dimeric rings. Smaller rings have only one likely anion binding site, while larger rings have two structural fragments suitable for hydrogen bonding with guests, thus providing the possibility for encapsulating two guest molecules or ions. To our knowledge, this is the first study that compares the anion binding properties of products from [1 + 1] and [2 + 2] cyclizations, thus preserving the same type and arrangement of the donor atoms and limiting variables only to size and shape of the macrocyclic ring. The only studies pursuing a similar approach published to date compared solid state adducts of chloride ions with a tetralactame and an octalactame host formed by condensation of 2,6-pyridinedicarboxylic acid ester and ethylenediamine in a [2 + 2] and [4 + 4] fashion, respectively,[15,25] but no data for host–guest association in solution have been reported.

(9) Kral, V.; Andrievsky, A.; Sessler, J. L. *J. Am. Chem. Soc.* **1995**, *117*, 2953–2954.
(10) Martinez-Manez, R.; Sancenon, F. *Chem. Rev.* **2003**, *103*, 4419–4476.
(11) Schmidtchen, F. P.; Berger, M. *Chem. Rev.* **1997**, *97*, 1609–1646.
(12) Bowman-James, K. *Acc. Chem. Res.* **2005**, *38*, 671–678.
(13) Choi, K.; Hamilton, A. D. *Coord. Chem. Rev.* **2003**, *240*, 101–110.
(14) Kang, S. O.; Hossain, M. A.; Bowman-James, K. *Coord. Chem. Rev.* **2006**, *250*, 3038–3052.
(15) Chmielewski, M. J.; Jurczak, J. *Chem. Eur. J.* **2005**, *11*, 6080–6094.
(16) Kang, S. O.; Powell, D.; Bowman-James, K. *J. Am. Chem. Soc.* **2005**, *127*, 13478–13479.
(17) Jadhav, V. D.; Schmidtchen, F. P. *J. Org. Chem.* **2008**, *73*, 1077–1087.
(18) Ghosh, S.; Choudhury, A. R.; Row, T. N. G.; Maitra, U. *Org. Lett.* **2005**, *7*, 1441–1444.
(19) Hossain, M. A.; Kang, S. O.; Powell, D.; Bowman-James, K. *Inorg. Chem.* **2003**, *42*, 1397–1399.
(20) Kavallieratos, K.; Bertao, C., M.; Crabtree, R. H. *J. Org. Chem.* **1999**, *64*, 1675–1683.
(21) Bondy, C. R.; Loeb, S. J. *Coord. Chem. Rev.* **2003**, *240*, 77–99.
(22) Gale, P. A. *Acc. Chem. Res.* **2006**, *39*, 465–475.
(23) Best, M. D.; Tobey, S. L.; Anslyn, E. V. *Coord. Chem. Rev.* **2003**, *240*, 3–15.
(24) Amendola, V.; Esteban-Gomez, D.; Fabrizzi, L.; Licchelli, M. *Acc. Chem. Res.* **2006**, *39*, 343–353.
(25) Szumna, A.; Jurczak, J. *Helv. Chim. Acta* **2001**, *84*, 3760–3765.

We have designed 14-, 15-, and 30-membered macrocycles containing both amide and amino groups (**1**, **2a**, **2b**, **4**, and **4m**, respectively, Scheme 1) capable of binding small molecules and anions. The 2,6-bis(carbamoyl)pyridine fragment was chosen because of its well-established anion recognition properties.[13,21,26] Having two distinct sites in one molecule, one of which could be used for other purposes such as a metal binding site,[27–29] can eventually lead to the design of a functional system with selectivity toward specific substrates. The designed macrocycles have additional amino groups that can act as H-bond donors/acceptors to enhance binding. These H-bond donors were shown to enhance the selectivity of polyfunctional guest binding. The importance of hydrogen bond donor abilities for efficient binding was demonstrated by substituting NH for NCH_3 and comparing the host **4** to its N-methylated analogue **4m**.

We have probed guest binding properties of our macrocyclic hosts with several kinds of guests: solvents that are H-bond acceptors (DMSO), solvents that are both H-bond donors and H-bond acceptors (MeOH), inorganic anions, monofunctional and difunctional carboxylates, and carboxylic acids. In our previous report we discussed the influence of topicity on fluoride binding to **4**.[6] Here we present the full account of this work as well as our findings on selective binding of carboxylates and carboxylic acids by 30-membered macrocycles **4** and **4m**, together with structural data on the interactions of carboxylic acids with the diaminodiamidopyridine motif.

Results and Discussion

Macrocycle **1** has been synthesized by a simple [1 + 1] condensation of 1,4,7,10-tetraazadecane and 2,6-pyridine dicarboxylic acid ester (Scheme 1).[30] Compounds **2a** and **2b** can be obtained by using an analogous approach; however, for **2b**, an alternative reaction with 2,6-pyridine dicarboxylic acid chloride[31] produced the product in much higher yield. Macrocycle **4** has been synthesized according to Scheme 1.

To make sure that the final product of [2 + 2] condensation did not contain any impurity of the [1 + 1] condensation product, the product of [2 + 1] condensation, **3**, was isolated and purified and only then reacted with an additional 1 equiv of 1,4,7,10-tetraazadecane, giving the final macrocycle **4** in a 10% overall yield. To study effects of substitution at the secondary amino groups we have also prepared a methylated derivative of **4**—macrocycle **4m**.

All synthesized ligands were characterized structurally. Structural data provide us with an insight into the binding mode of small molecules to the macrocyclic hosts. Compound **1** does not incorporate solvent molecules in the solid state (crystallization from alcohols, acetonitrile, chloroform, or methylene chloride invariably yielded the same solvent-free structure). The rigid 2,6-bis(carbamoyl)pyridine fragment induced the nearly planar shape for both the 15-membered macrocycle **1**[30] and the 14-membered macrocycles **2a** and **2b** (Figures S1 and S2, Supporting Information).

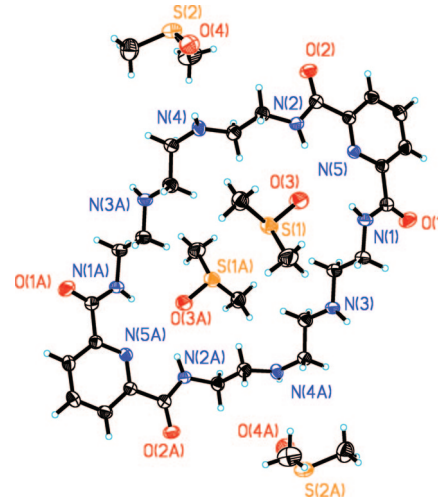

FIGURE 1. ORTEP plot of **4·2DMSO**.

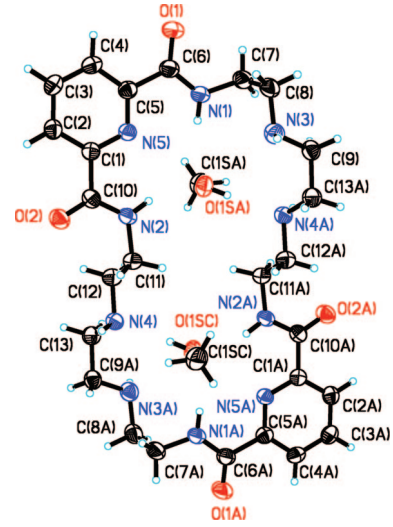

FIGURE 2. ORTEP plot of **4·2MeOH**.

Compound **4**, which has a large [2 + 2] ring, binds two molecules of either DMSO or methanol, giving rise to two different conformations of the ring.

In the case of DMSO, each of the two DMSO molecules forms two hydrogen bonds with two amide groups (Figure 1, Figures S3 and S4, Supporting Information). The overall conformation of the macrocylic cavity resembles the shape of the previously described macrocycles with α,ω-diamino linkages.[15] The chains linking 2,6-bis(carbamoyl)fragments are essentially unstrained, with NCCN torsional angles close to optimal 180° and 60°. Parameter *h*, introduced by Chmielewski and Jurczak[15] to describe the distance between the planes of the two pyridine rings in the molecules, is 5.79 Å, which falls into a general trend for macrocycles with aliphatic linkers (Figure S5, Supporting Information). NH groups of the linker in **4·2DMSO** form intermolecular hydrogen bonds with amide groups resulting in a sheet-like structure (Figure S6, Supporting Information).

Binding of methanol by **4** is different because of the ability of MeOH to form three hydrogen bonds. The presence of additional hydrogen bonding sites (NH groups) leads to a completely different conformation (Figure 2). The linkers are still almost unstrained, but the macrocycle adopts a bicompartmental structure with three hydrogen-bonding sites for each

(26) Kang, S. O.; Begum, R. A.; Bowman-James, K. *Angew. Chem., Int. Ed.* **2006**, *45*, 7882–7894.
(27) Mascharak, P.; Marlin, D. *Chem. Soc. Rev.* **2000**, *29*, 69–74.
(28) Korendovych, I. V.; Kryatova, O. P.; Reiff, W. M.; Rybak-Akimova, E. V. *Inorg. Chem.* **2007**, *46*, 4197–4211.
(29) Ghosh, S.; Roehm, B.; Begum, R. A.; Kut, J.; Hossain, M. A.; Day, V. W.; Bowman-James, K. *Inorg. Chem.* **2007**, *46*, 9519–9521.
(30) Korendovych, I. V.; Staples, R. J.; Reiff, W. M.; Rybak-Akimova, E. V. *Inorg. Chem.* **2004**, *43*, 3930–3941.
(31) Voegtle, F.; Weber, E.; Wehner, W.; Naetscher, R.; Gruetze, J. *Chem.-Ztg.* **1974**, *98*, 562–563.

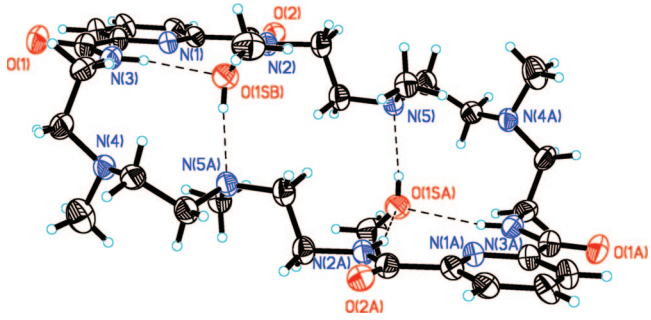

FIGURE 3. ORTEP plot of **4m·2MeOH**.

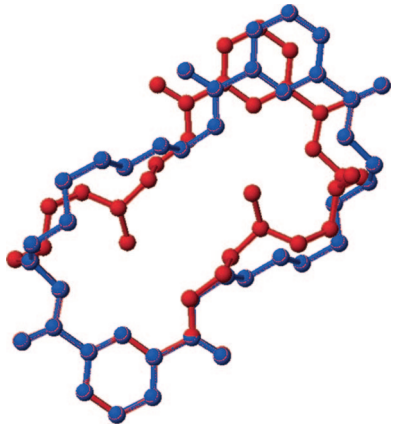

FIGURE 4. Overlay of crystal structures of **4** (blue) and **4m** (red). Methanol molecules and hydrogen atoms are omitted for clarity; view is along the axis perpendicular to the plane of the pyridine ring.

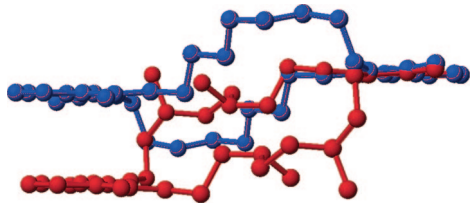

FIGURE 5. Overlay of crystal structures of **4** (blue) and **4m** (red). Methanol molecules and hydrogen atoms are omitted for clarity; view is along the plane of the pyridine ring.

methanol molecule. The host oxygen atom is in a nearly tetrahedral environment provided by the hydrogen bonds. The two pyridine ring planes are nearly coplanar and separated by 0.65 Å. We call the resulting conformation "Z-conformation" (Figure S7, Supporting Information). Methanol binding in the solid state is reversible: upon standing in chloroform solution **4·2MeOH** loses methanol and precipitates as pure **4**, as evidenced by the NMR data.

Methylation of the secondary amine nitrogens has a profound effect on the structure of the molecule. Although the linkers in **4m** remain unstrained as evidenced by the values of torsion angles similar to nearly ideal ones described above for **4**, the structure of **4m** (Figure 3) is quite different from that of **4**. The differences can be clearly seen on the overlay of the two structures (Figures 4 and 5); two of the methyl groups that were absent in **4** are pointing inside the cavity in **4m**, and the distance between the planes of the pyridine rings is now 3.89 Å compared to a much shorter distance of 0.65 Å in **4**. Altogether, the introduction of methyl groups creates additional steric bulk in the cavity of the macrocyclic ring. Nevertheless, **4m** also can bind two molecules of methanol in the same fashion as **4**.

Anions can be expected to bind with hosts **1**−**4** stronger than neutral solvent molecules. The interaction of **1**, **4**, and **4m** with dihydrogen phosphate and hydrogen sulfate ions was studied to test this hypothesis. The 15-membered macrocycle **1** does not bind $H_2PO_4^-$ or HSO_4^-, whereas both **4** and **4m** show significant affinity toward these anions (Table 1). Introduction of methyl groups in **4m** leads to a decrease in binding constants in all cases. Interestingly, binding of HSO_4^- is much more sensitive to methylation of secondary amino groups than $H_2PO_4^-$: in the latter case, the association constant for **4m** is ~2 times smaller compared to that of **4**, whereas in the former case, it drops by 2 orders of magnitude. In addition to an increase in steric bulk, the lack of hydrogen atoms on the amine NH groups can have a negative effect on the HSO_4^- binding. Comparison of the binding constants with the literature data also provides interesting insight into the importance of amino groups adjacent to the amidopyridine fragment. Closely related macrocylic amides studied by Jurczak and Chmielewski,[15] where two amidopyridine fragments were linked by a pair of hydrocarbon chains, showed much lower affinity (maximum value of association constant was 75 M^{-1}) for hydrogen sulfate anion than **4** (Table 1). Interestingly, the value reported by Jurczak and Chmielewski[15] corresponds well to the binding constant of HSO_4^- to **4m**, suggesting that the anion binding in this case is mostly the result of interactions of hydrogen sulfate anion with the amide NH groups. Comparison of the reported data on $H_2PO_4^-$ and monocarboxylates with our data for **4** is less straightforward, since a profound influence of the ring size on the binding was observed.[15] Unfortunately, the largest macrocycle in that study was 24-membered, so no direct comparison can be made with 30-memberered **4** and **4m**. The affinity of **4** to HSO_4^- is in fact the highest among reported neutral mono- and bicyclic amino-amide macrocycles[14] and is only 50% smaller than that of the quarternized receptor developed by Bowman-James and co-workers.[19]

Chloride ion is only weakly bound by **4**, whereas I^- and noncoordinating anions such as ClO_4^- and PF_6^- showed essentially no binding. This observation is also indirectly confirmed by the crystal structure of **1·HClO₄**: no H-bonding of perchlorate oxygens to the 2,6-bis(carbamoyl)fragment is observed in the solid state (Figures S8 and S12, Supporting Information).

The 1:1 stoichiometry of binding of dihydrogen phosphate or hydrogen sulfate with **4** or **4m** was confirmed by the corresponding Job's plots (Figures S17 and S20, Supporting Information). However, large macrocycles, such as 30-membered **4** and **4m**, can potentially bind several anions. Therefore we have undertaken a study of the influence of the macrocycle ring size on topicity of **4** and **4m**.

Smaller rings (e.g., **1**) have only one likely anion binding site, while larger rings have two structural fragments suitable for hydrogen bonding with guests, thus providing the possibility for encapsulating two guest molecules or ions. The smallest anion, F^-, was used to probe the effects of the macrocyclic ring size. The 15-membered [1 + 1] macrocycle **1** is capable of binding F^- ions, as determined by NMR titration with NBu_4F.

(32) Hynes, M. J. *J. Chem. Soc., Dalton Trans.* **1993**, 311–312.
(33) Boiocchi, M.; Boca, L. D.; Esteban-Gomez, D.; Fabrizzi, L.; Licchelli, M.; Monzani, E. *Chem. Eur. J.* **2005**, *11*, 3097–3104.
(34) Kang, S. O.; Hossain, M. A.; Powell, D.; Bowman-James, K. *J. Am. Chem. Soc.* **2004**, *126*, 12272–12273.
(35) Camiolo, S.; Gale, P. A.; Hursthouse, M. B.; Light, M. E. *Org. Biomol. Chem.* **2003**, *1*, 741–744.

TABLE 1. Summary of Binding Constants of 4 and 4m with Different Anions and Carboxylic Acids

guest	association constant for **4**, M^{-1}	chemical shift of **4**·**guest**, ppm	association constant for **4m**, M^{-1}	chemical shift of **4m**·**guest**, ppm
$H_2PO_4^-$	$1.0(1) \times 10^3$	11.00(3)	$4.3(5) \times 10^2$	10.35(3)
HSO_4^-	$4(2) \times 10^3$	10.55(3)	38(2)	10.84(3)
F^-	$K_1 = 4(7) \times 10^3$	11.2(5) − 1:1	$K_1 = 1.0(4) \times 10^4$	12.4(2) − 1:1
	$K_2 = 3(5) \times 10^2$	12.39(7) − 1:2	$K_2 = 3(7) \times 10^3$	12.31(2) − 1:2
Cl^-	28(2)	9.80(2)		
I^-	<10			
PF_6^-	no binding			
ClO_4^-	no binding			
		carboxylic acids		
acetic	23(3)	9.98(3)		
benzoic	$1.5(1) \times 10^2$	9.91(1)		
oxalic	precipitate formation			
malonic	$8(2) \times 10^1$	9.86(4)		
succinic	$5(2) \times 10^3$	10.18(2)	11(3)	9.50(5)
malic			$1.25(5) \times 10^2$	9.458(3)
glutaric	$2.1(2) \times 10^3$	10.316(6)	11(3)	9.49(4)
2-metylglutaric			8(2)	9.50(5)
adipic	$3.9(2) \times 10^2$	10.164(9)		
sebacic	68(3)	9.89(1)		
maleic	<10			
fumaric	$>10^5$	10.8(1)	$1.63(7) \times 10^2$	9.803(6)
		carboxylates		
TEA benzoate	35(1)	10.13(1)		
TBA acetate	88(2)	10.37(1)	42(3)	10.46(4)
TEA oxalate	$1.3(1) \times 10^3$	11.03(1)		
TEA malonate	$6(1) \times 10^3$	11.12(2)		
TEA succinate	$3(1) \times 10^4$	11.20(1)	$4.5(6) \times 10^2$	11.14(2)
TEA glutarate	$1.2(2) \times 10^3$	11.11(4)		
TEA sebacate	$6(1) \times 10^2$	10.26(4)		
TEA maleate	$2.5(9) \times 10^4$	11.06(3)		
TEA fumarate	$5.7(3) \times 10^3$	10.985(5)		
TEA tartrate	$5.1(5) \times 10^2$	10.43(2)		

Nonlinear least-squares fit of the resulting titration curve with the program Wineqnmr[32] yielded an assosiation constant of $K = 5.8(7) \times 10^2\ M^{-1}$ (Figure S21, Supporting Information). The 1:1 stoichiometry of the interaction was unambiguously established by using Job's plot (Figures S22 and S23, Supporting Information).

Large excess of fluoride ions leads to deprotonation of **1** to form HF_2^- and DF_2^- ions, as evidenced by a doublet (−143.4 ppm, $^1J(H,F) = 119$ Hz) and a triplet (−143.8 ppm, $^1J(D,F) = 18$ Hz), respectively, in the ^{19}F spectrum. Similar observations were reported by Chmielewski and Jurczak[15] and by others[33–35] for their hosts. After several days, the signal of HF_2^- completely disappears and only the peak for DF_2^- is present, due to the fluoride-facilitated deuterium exchange between DMSO-d_6 and the ligand. The fluoride-binding properties of the 14-membered macrocycles **2a** and **2b** differ drastically from those of **1**: **2a** and **2b** do not bind fluoride. It can be concluded that at least a 15-membered macrocycle is needed for encapsulating fluoride anion in 2,6-bis(carbamoyl)-containing hosts.

For the larger cavity macrocycle **4**, the corresponding Job's plot has a maximum at a 1:2 ratio of ligand to fluoride (Figure S24, Supporting Information). To clarify the stoichiometry of the binding of fluoride ion to **4**, we have also performed NMR titrations in solution. The titration curve of **4** with NBu_4F, in agreement with previously reported results,[15] has a sigmoidal shape, which may be indicative of the formation of two species. Extracting quantitative binding affinities for the 1:1 and 1:2 complexes of **4** with fluoride, however, was hampered by experimentally observed dependence of the data (in terms of both the shape of the curve and quantitative fitting parameters) on initial concentrations of reagents. Additional experiments showed that variable concentration of water is the reason for such inconsistency. For example, position of the amide peak at [**4**]/[F^-] = 1:2 shifts by 1 ppm upon increasing water content from 20 to 110 equiv! The same effect was observed for binding of fluoride to **1** in the presence of water. Water is inherently present in all tetrabutylammonium fluoride solutions prepared from commercially available aqueous NBu_4F, and different amounts of water are added in standard titrations of macrocyclic host with fluoride solutions. This "water effect" might explain why in many cases[15,19] binding of fluoride to the receptor could not be modeled adequately.

The pronounced influence of water on fluoride binding to amidopyridine macrocycles suggested that further studies of fluoride binding to macrocyclic hosts have to be done under carefully controlled conditions. Since anhydrous NBu_4F is unstable,[36] water could not be completely excluded from the system. Instead, we decided to perform titration under constant water concentration (ca. 250 mM). Qualitatively the observed sigmoidal shape can be explained by competitive binding of fluoride and water. Quantitative modeling of multiple equilibria in this system required extensive systematic variations of both H_2O and F^- concentrations, and was beyond the scope of the present work. As has been shown by Bowman-James and coworkers,[37] the situation can be further complicated by significant affinity of ditopic guest to bifluoride. However, fitting of the region where fluoride binding dominates can provide us with

(36) Sun, H.; DiMagno, S. G. *J. Am. Chem. Soc.* **2005**, *127*, 2050–2051.
(37) Kang, S. O.; Powell, D.; Day, V. W.; Bowman-James, K. *Angew. Chem., Int. Ed.* **2006**, *45*, 1921–1925.

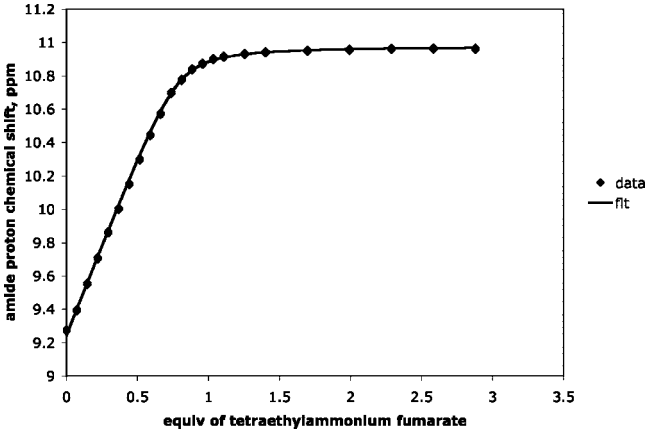

FIGURE 6. Titration curve (following chemical shift of the amide protons of the macrocycle) of **4** (10 mM) with tetraethylammonium fumarate (100 mM) in DMSO-d_6 at 20 °C. Binding parameters determined by program Wineqnmr are δ(complex) = 10.985(5) ppm, association constant $K = 5.7(3) \times 10^3$ M^{-1}.

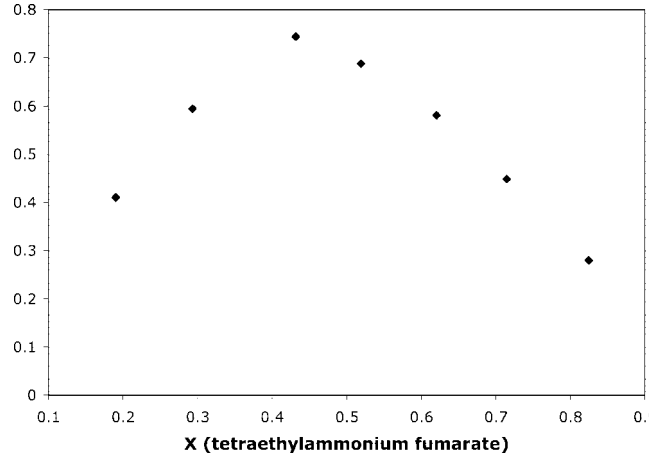

FIGURE 7. Job's plot of **4** and tetraethylammonium fumarate in DMSO-d_6 at 20 °C (total concentration 10 mM), showing 1:1 stoichiometry of binding. The chemical shift of the amide protons of the macrocycle was followed.

an estimate of the binding constants. This region of the curve (Figure S25, Supporting Information) can be fit both with 1:1 and 1:2 models; however, the 1:2 model provides a better fit ($K_1 = 4(7) \times 10^3$ M^{-1}, $K_2 = 3(5) \times 10^2$ M^{-1}, $R = 0.31\%$) than the 1:1 model ($K = 3.7(3) \times 10^2$ M^{-1}, $R = 0.44\%$). The binding occurs under fast exchange conditions, so no splitting (both in ^{1}H and ^{19}F NMR spectra) as a result of anion binding was observed.

Studies of binding of F$^-$ to **4m** conducted in an analogous manner (under constant water concentration of ca. 250 mM, Figure 26, Supporting Information) also displayed the sigmoidal shape of the titration curve indicative of a 1:2 complexation, and showed that the presence of extra methyl groups does not negatively affect the association constant (Table 1). In fact, the overall binding constant is about an order of magnitude larger: $K_1K_2 = 4(3) \times 10^7$ M^{-2} for **4m** as opposed to $K_1K_2 = 1(3) \times 10^6$ M^{-2} for **4**.

The values of stepwise fluoride binding constants, K_1 and K_2, determined in this work for fluoride binding to **4** or **4m** are similar to those obtained by Bowman-James and co-workers for a 1:1 F$^-$ complexation with closely related 24-membered macrocycles (log K values of 2.61 and 2.04),[19] showing small dependence of fluoride binding affinity on the presence of additional H-bond donors and the ring size at the same time retaining strong selectivity for fluoride over the other halides.

To further explore molecular recognition properties of **4** and **4m**, we have studied binding of tetraethylammonium salts of mono- and dicarboxylic acids. Monocarboxylates are only weakly bound by **4** and **4m** (Table 1). However, going from a monocarboxylate to a dicarboxylate (e.g., tetraethylammonium fumarate) improves binding affinities to up to 3 orders of magnitude (Table 1 and Figure 8). A representative NMR titration curve is shown in Figure 6. The Job's plot unambiguously proves the 1:1 binding mode of dicarboxylate to the macrocycle (Figure 7). This suggests ditopic binding of the dicarboxylate to **4** in solution. We have also observed that **1**, **2a**, and **2b** do not bind benzoate or fumarate, suggesting that higher flexibility and the presence of additional secondary amino groups and/or an additional amidopyridine moiety in the larger ring are essential for binding of carboxylates. We have studied the effect of chain length on binding of dicarboxylates and found a strong dependence of the binding constant on the chain length

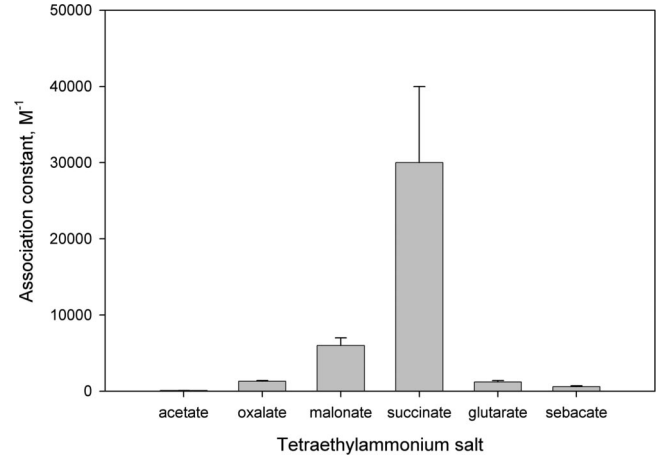

FIGURE 8. Association constants for selected carboxylic acids salts with the macrocyclic host **4**.

(Table 1 and Figure 8). Importantly, pK_a values of all but the shortest dicarboxylic acids are very close to each other (Table 2), so that the observed selectivity cannot be attributed to differences in basicity of dicarboxylate anions.

Succinate has the largest binding constant, followed by malonate. The four-carbon chain seems to be optimal for efficient binding of dicarboxylic acids. Once the linker length is not optimal, the value of binding constant drops almost to the values exhibited by monocarboxylates. An analogous effect was previously observed for polyamine receptors by Hosseini and Lehn.[38]

To probe the geometric selectivity of the binding we have determined association constants of **4** with tetraethylammonium fumarate and maleate. Even though the K_a was large in both cases, only modest selectivity for maleate was observed (Table 1).

Incorporation of amino groups in the molecule can potentially facilitate anion binding because of the protonation of the nitrogen atoms. These effects were extensively studied in polyammonium receptors.[39] Size and shape complementarity were found to be the key factors in the development of such

(38) Hosseini, M. W.; Lehn, J.-M. *Helv. Chim. Acta* **1986**, *69*, 587–603.
(39) Llinares, J. M.; Powell, D.; Bowman-James, K. *Coord. Chem. Rev.* **2003**, *240*, 57–75.

TABLE 2. pK_a Values for Different Acids in Water in DMSO[a]

acid	pK_a(water)	pK_a(DMSO)
acetic	4.756	12.3
benzoic	4.204	11.1
oxalic	1.25, 3.81	6.2, 14.9
2-oxobutyric	2.50	
malonic	2.85, 5.70	7.2, 18.5
succinic	4.21, 5.64	9.5, 16.7
glutaric	4.32, 5.42	10.9, 15.3
adipic	4.41, 5.41	11.9, 14.1
sebacic	4.59, 5.59	
maleic	1.92, 6.23	
fumaric	3.02, 4.38	9.2, 11.2
2-ketoglutaric	2.47, 4.68	
malic	3.40, 5.11	
D-tartaric	2.98, 4.34	8.1, 12.2
$DTBPH^+$	4.95	0.81
H_2SO_4	–3.0, 1.99	pK_2 = 9.1
H_3PO_4	2.12, 7.21, 12.32	
HF	3.17	15
HCl	–8.0	1.8
HI	–10.0	0.9
H_2O	15.7	32

[a] Values for carboxylic acids in DMSO are taken from ref 45 and 46, values for carboxylic acids in water are from the CRC Handbook of Chemistry and Physics (84th edition 2003−2004), values for inorganic acids are from ref 47, and pK_a values for DTBPH are taken from ref 41.

receptors.[38,40]Therefore we set out to explore the binding of carboxylic acids by **4** and **4m**. Intermolecular H-bonding between −COOH groups and secondary amino groups of the macrocycle was expected to enhance binding and to possibly provide selectivity.

In the case of dicarboxylic acid binding to hosts containing basic amino groups, chemical shift changes can originate from simple protonation of the macrocycle. To separate these contributions, control experiments were performed, which allowed us to investigate effects of protonation on chemical shifts of the macrocycle. We selected 2,6-di-*tert*-butylpyridinium hexafluorophosphate ($DTBPHPF_6$) as our proton source; $DTBPHPF_6$ is fairly acidic in DMSO[41] (pK_a = 0.81, Table 2) and can be conveniently used to prepare solutions of known concentration in the absence of water. Independent experiments (vide supra) established that hexafluorophosphate anions do not bind to the macrocycle. The results of titration of **4** and **4m** with $DTBPHPF_6$ are presented in Figures S39−S42, Supporting Information. As can be seen from the chemical shift of the 2,6-di-*tert*-butylpyridinium protons, macrocycle **4** is completely protonated upon addition of 4 equiv of acid. The corresponding changes of chemical shifts of the amide proton are more complex: initially, the amide proton chemical shift changes from 9.29 ppm to 9.30 ppm upon addition of 1 equiv of acid, then it drops to 9.27 ppm at 2 equiv of H^+, and finally reaches the maximum value at 9.38 ppm for the tetraprotonated species. The corresponding titration curve for **4m** shows slightly larger overall chemical shift changes, but the final chemical shift of amide protons does not exceed ca. 9.39 ppm for the tetraprotonated species. The magnitude of change of the chemical shift observed in these experiments (∼0.15 ppm) is several times smaller than typical values observed in titrations of **4** and, to a smaller extent, in titrations of **4m** with carboxylic acids (Table 1). Therefore, the NMR spectral changes observed in the course

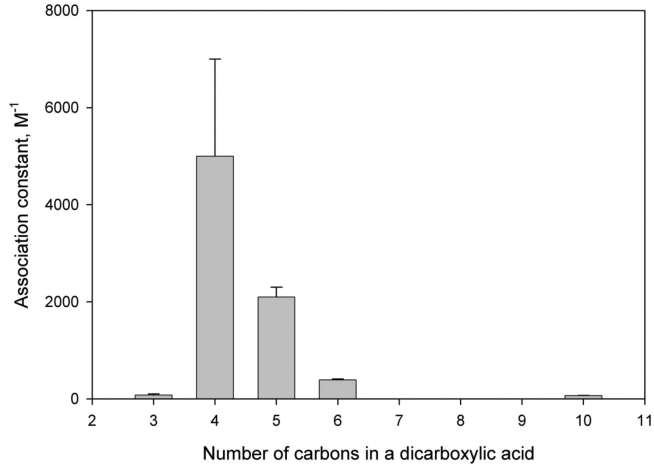

FIGURE 9. Dependence of the equilibrium constant of dicarboxylic acid binding to **4** on the number of carbon atoms.

of reactions between **4** or **4m** and dicarboxylic acids cannot be solely attributed to the protonation of macrocyclic hosts (vide infra).

The behavior of carboxylic acids upon binding with **4** and **4m** agrees well with that of their salts (Figure 9). We have studied binding of a variety of different mono- and dicarboxylic acids and found a very significant dependence of the binding constant on the nature of the carboxylic acid. The results of these binding studies are summarized in Table 1. Importantly, Job's plots show a 1:1 stoichiometry of binding of dicarboxylic acids (Figure S52, Supporting Information).

Binding of monocarboxylic acids is generally weaker than that of dicarboxylic acids, which is consistent with the trend observed for the carboxylates. On the other hand, the difference between binding constants for different dicarboxylic acids is drastic (Table 1). It can be best illustrated with simple aliphatic dicarboxylic acids, where binding constants clearly depend on the linker length, reaching a maximum for succinic acid.

To further investigate this effect for our amide-containing macrocycles, we have studied binding of rigid guests with optimal chain length: maleic and fumaric acids. The results of this study turned out to be very interesting: the binding constant for fumaric acid was found to be higher than the upper limit of NMR determination ($>10^5$ M^{-1}), whereas the binding of maleic acid is extremely weak ($K < 10$ M^{-1}) and results primarily from the protonation of the macrocycle as evidenced by the small magnitude of the chemical shift of the amide proton.

Such a drastic difference in binding of fumaric and maleic acids vs. their tetraethylammonium salts deserved further investigation, therefore we have conducted binding studies in the presence of constant amounts of a strong acid added prior to the addition of anionic titrant. In a typical experiment several equivalents of $DTBPHPF_6$ were added to the solution of host in DMSO prior to the addition of tetraalkylammonium carboxylate. This approach can help separate contributions of the protonation and dicarboxylate binding to the chemical shifts.

The titration curve of **4** with tetraethylammonium fumarate in the presence of 2 equiv of noncoordinating acid is presented in Figure 10. It represents strong binding with a 1:1 stoichiometry (the association constant is $6(3) \times 10^3$ M^{-1}, chemical shift of the complex is 10.88 ppm). In the case of titration of **4** with tetraethylammonium fumarate in the presence of 4 equiv of the acid an initial lag period is observed (Figure 10) followed by a sharp rise in chemical shift of the amide protons after

(40) Carvalho, S.; Delgado, R.; Fonseca, N.; Felix, V. *New J. Chem.* **2006**, *30*, 247–257.
(41) Benoit, R. L.; Frechette, M.; Lefebvre, D. *Can. J. Chem.* **1988**, *66*, 1159–1162.

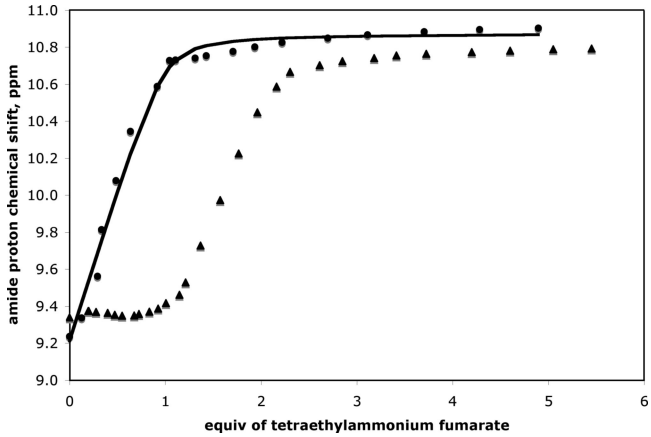

FIGURE 10. Titration curve (following chemical shift of the amide protons of the macrocycle) of **4** (10 mM) with tetraethylammonium fumarate (100 mM) in DMSO-d_6 at 20 °C in the presence of 2 equiv of $DTBPHPF_6$ (circles) and 4 equiv of $DTBPHPF_6$ (triangles).

addition of ca. 1 equiv of the titrant. Such dependence suggests that diprotonated host displays the maximum affinity to the fumarate guests. The lag in titration curve can be explained by initial protonation of the dicarboxylate by 2 equiv of acid followed by subsequent binding of the fumarate to the diprotonated molecule of the host.

Importantly, the spectra suggest that the bound fumarate is closely associated with protonated nitrogen atom protons, i.e., the chemical shift of the fumarate immediately upon addition to diprotonated **4** almost reaches the value for the free fumaric acid, being constant until 1 equiv of the salt is added, at which point it gradually decreases back due to fast exchange with the unbound fumarate (Figure S53, Supporting Information).

The titration curves of **4** with tetraethylammonium maleate in the presence of acid are very different from those of fumarate (Figure S54, Supporting Information). No immediate strong binding of the dicarboxylate was observed with either 2 or 4 equiv of H^+. When 2 equiv of strong acid were added before the titration, the signals of the amide protons of the host only started to shift after addition of 2 equiv of the dicarboxylate. Analogous behavior was observed in the case when 4 equiv of acid was added prior to titration. In both cases binding occurred only when maleate dianion was present in solution, and no appreciable binding of hydrogen maleate was observed. Under these conditions, neutral macrocycle acted as a host. The protonation state of maleic acid can be followed by its chemical shift. Upon addition of ca. 2 equiv of tetraethylammonium maleate, only the signal corresponding to hydrogen maleate is present. Then a signal corresponding to bound maleate dianion appears. The spectra show that hydrogen maleate and maleate are in slow exchange on the NMR time scale.

In a control experiment with no macrocycle present we have also observed slow exchange between the different protonation states of the maleic acid (with the chemical shifts of 5.18, 6.01, and 6.28 ppm for TEA maleate, TEA hydrogen maleate, and maleic acid, correspondingly) (Figure S55, Supporting Information). The protonation state of the host and the guest in the tight adduct between **4** and maleate was confirmed by reverse titrations of the **4**:maleate complex (at the 1:2 stoichiometry) with noncoordinating acid (Figure 11).

The gradual addition of $DTBPHPF_6$ to the complex of **4** with maleate results in a disappearance of the peak of the maleate and an appearance of a peak corresponding to hydrogen maleate with concurrent decrease of the amide proton chemical shift. These data are clearly consistent with the lack of binding of maleic acid or hydrogen maleate to **4**, and suggest strong binding of doubly deprotonated maleate to **4**.

Such a drastic difference between the association of **4** with fumaric/maleic acid vs their corresponding salts may suggest the importance of the guest geometry for its efficient molecular recognition by **4** in its protonated state. Alternatively, the different behavior of maleic acid can be explained by a much higher stability of the hydrogen maleate anion, which is stabilized by an internal hydrogen bond. Therefore the monodeprotonated maleic acid is unable to bind strongly to the macrocycle. In the absence of direct structural evidence, it is difficult to favor one of these possibilities over the other.

Important insight into the binding mode of fumarate and succinate can be obtained from previously published crystal structures of a related bis-isophthalamide macrocycle forming rotaxanes with fumaric and succinic acid derivatives.[42–44] Fumaramide derivatives served as very efficient preorganization templates for rotaxane synthesis, and their rigid configuration around the double bond was essential for binding as followed from the crystal structures. The succinamide linker in the rotaxane structure adopted a trans conformation in order to form hydrogen bonds between the amide hydrogen atoms of the isophthalamide macrocycle and the C═O group of the linker.

X-ray crystallographic studies of the adducts of macrocyclic hosts with different anions provided great insight into the binding mode of guests with macrocyclic hosts,[12,14] and may also shed light on the binding modes of dicarboxylic acids. We were able to obtain crystals of a 1:2 adduct of **4** with glutaric acid from a water–methanol−chloroform biphasic mixture. Because crystallization was performed in the presence of a substantial amount of water, which is known to bind strongly to the 2,6-bis(carbamoyl)pyridine fragment, this particular crystal structure might not accurately represent the structures of carboxylic acid adducts with **4** detected by NMR in DMSO solution studies.

The 1:2 adduct, $\mathbf{4 \cdot 2(CH_2)_3(CO_2H)_2}$, has been crystallized with nine water molecules per asymmetric unit. The water molecules support an extensive three-dimensional network of hydrogen bonds. Two of the water molecules are bound to the 2,6-bis(carbamoyl)fragments. Each molecule of the carboxylic acid is bound by hydrogen bonds to the amino groups, resulting in the conformational change of the macrocyclic ring. The molecules of glutaric acid form "bridges" between the molecules of **4**, creating infinite chains that are additionally supported by water molecules (Figure 12). Similar binding was observed by Bowman-James et al. for polyamine macrocycle complexes with sulfate and nitrate ions.[48]

Much more insight into the binding mode of the carboxylic acid with the macrocyclic host **4** in nonaqueous solutions can

(42) Gatti, F. G.; Leigh, D. A.; Nepogodiev, S. A.; Slawin, A. M. Z.; Teat, S. J.; Wong, J. K. Y. *J. Am. Chem. Soc.* **2001**, *123*, 5983–5989.
(43) Marlin, D.; Cabrera, D. G.; Leigh, D. A.; Slawin, A. M. Z. *Angew. Chem., Int. Ed.* **2006**, *45*, 1385–1390.
(44) Cooke, G.; Garety, J. F.; Jordan, B.; Kryvokhyzha, N.; Parkin, A.; Rabani, G.; Rotello, V. M. *Org. Lett.* **2006**, *8*, 2297–2300.
(45) Bordwell, F. G. *Acc. Chem. Res.* **1988**, *21*, 456–463.
(46) Izutsu, K. *Acid−Base Dissociation Constants in Dipolar Aprotic Solvents*. Blackwell Scientific Publications: Brookline Village, MA, 1990.
(47) Bjerrum, J. *Stability Constants*; Chemical Society: London, UK, 1958.
(48) Clifford, T.; Danby, A.; Llinares, J. M.; Mason, S.; Alcock, N. W.; Powell, D.; Aguilar, J. A.; Garcia-Espana, E.; Bowman-James, K. *Inorg. Chem.* **2001**, *40*, 4710–4720.

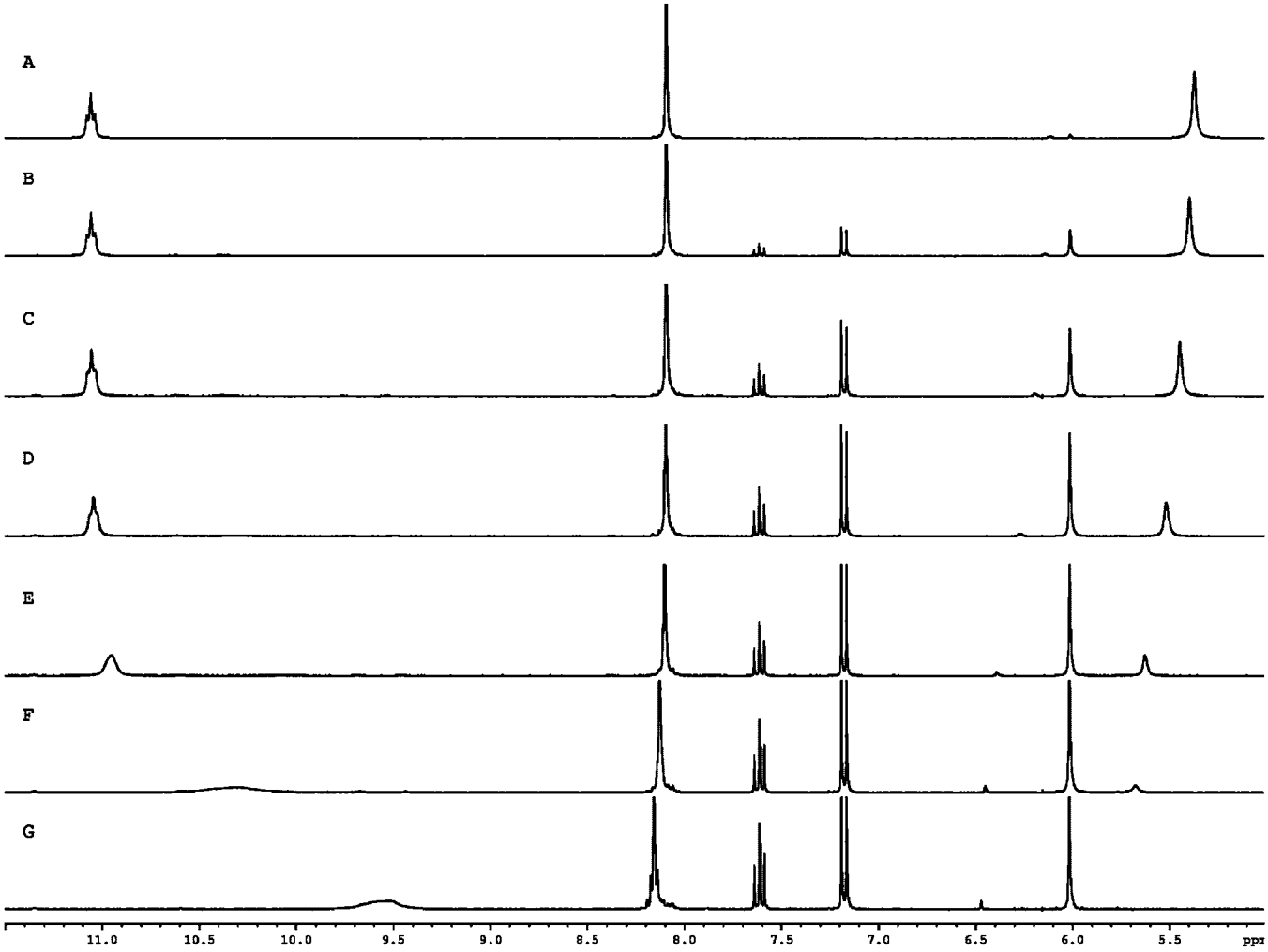

FIGURE 11. ^{1}H NMR spectra of the complex of **4** with tretraethylammonium maleate (2.3 equiv) upon addition of 0 (A), 0.3 (B), 0.7 (C), 1.0 (D), 1.5 (E), 2.0 (F), and 2.3 equiv (G) of $DTBPHPF_6$.

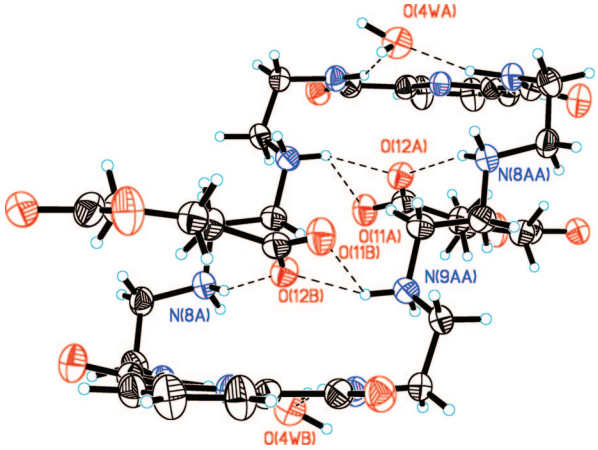

FIGURE 12. ORTEP plot of an adduct of $\mathbf{4}\cdot\mathbf{2(CH_2)_3(CO_2H)_2}$. Water molecules except for the ones bound to the amide nitrogens are omitted for clarity. Displacement ellipsoids are drawn at the 50% probability level.

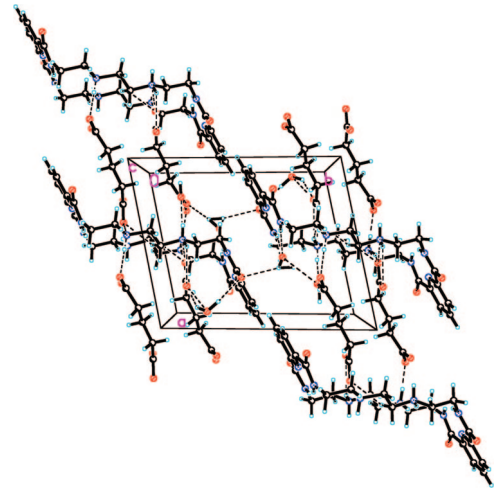

FIGURE 13. Packing diagram of $\mathbf{4}\cdot\mathbf{2(CH_2)_3(CO_2H)_2}$ viewed along the crystallographic *c* axis showing intermolecular hydrogen bonding.

be obtained from the crystal structure of the adduct of **4** with *p*-nitrobenzoic acid (Figure 13). This adduct can be precipitated from a solution of **4** in DMSO upon addition of excess *p*-nitrobenzoic acid. The crystal structure of the product shows four molecules of the carboxylic acid bound to the macrocycle. In the absence of a significant amount of water competing with the carboxylic acid, the 2,6-bis(carbamoyl)pyridine fragment binds one of the oxygen atoms of the guest carboxylate group, whereas the neighboring protonated amino group binds the other carboxylate oxygen in a chelating fashion (Figure 14). Such a binding mode clearly indicates the importance of neighboring

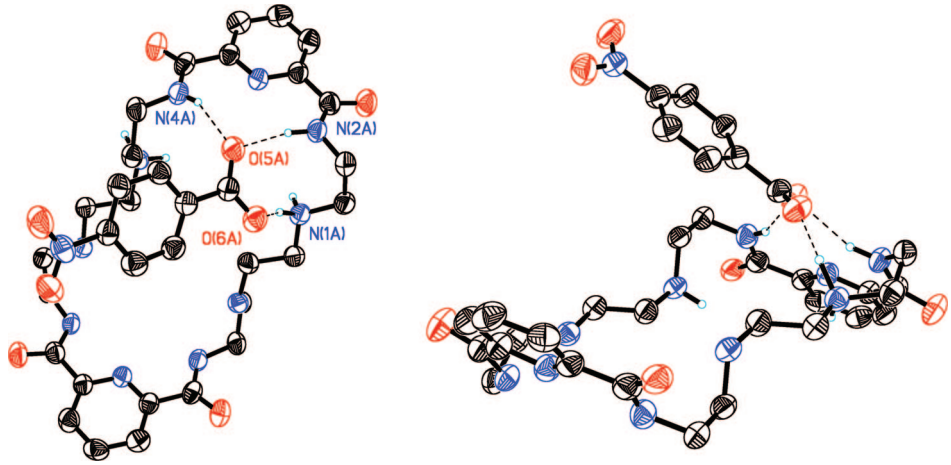

FIGURE 14. ORTEP plots of an adduct of **4**·**4**(**4**-$NO_2C_6H_4CO_2H$). DMSO molecules are omitted for clarity. Also only one molecule of *p*-nitrobenzoic acid is shown for clarity. Displacement ellipsoids are drawn at the 50% probability level.

amino groups in carboxylate recognition. The other carboxylic acid molecules bound to **4** in this structure form hydrogen bonds with two protonated amino groups in a similar fashion to **4**·**2**$(CH_2)_3(CO_2H)_2$.

The importance of shape complementarity for molecular recognition is further confirmed by studies of guest binding by **4m**, where these effects are additionally amplified. Generally, binding constants for **4m** are lower than those for **4** (Table 1), which is expected considering the more sterically hindered **4m** structure with fewer NH hydrogen atoms available for hydrogen bonding. This effect is best represented by the values of association constants for succinic and glutaric acids: they drop by ca. 2 orders of magnitude. In the case of **4m** the magnitudes of the chemical shifts for the dicarboxylic acids are also lower than those in the case of **4** (Figure S56, Supporting Information), so the binding affinity data have to be more carefully interpreted. In contrast to **4**, no significant chain length dependence was observed for **4m** (at least in part due to low values of the binding constants). Relatively small chemical shifts and low binding affinities of **4m** made exhaustive titrations with all possible guests not only technically difficult, but in many cases pointless, as no clear trends could be deduced from the data. The steric factors, however, are important in guest binding to **4m**. For example, steric bulk of the guest in the case of 2-methylglutaric acid can explain a somewhat lower binding constant of 8(2) M^{-1} compared to the other dicarboxylic acids.

The significant selectivity observed for fumaric and maleic acids is maintained for **4m**; it modestly binds fumaric acid with an association constant of $1.63(7) \times 10^2$ M^{-1} and a chemical shift of 9.803(6) ppm for the complex. At the same time, titration of **4m** with maleic acid proceeds with a much lower chemical shift change and is best fit with a 1:2 model showing small changes in chemical shifts, consistent with just protonation of the macrocycle (Figure S59, Supporting Information).

We have also probed the interaction of **4m** with functionalized dicarboxylic acids: α-keto and α-hydroxy acids. The lack of secondary amino group in **4m** allows for studying association of macrocycles with the guests containing more reactive functional groups, such as carbonyls. Introduction of additional H-bond donors/acceptors can result in stronger interaction between the macrocyclic host and the guest as well as potentially higher selectivity for certain types of guest molecules. Introduction of a hydroxy group to a carboxylic acid immediately results in an increase in the binding constant by ca. 1 order of magnitude (compare the results for malic and succinic acids, Table 1). A keto-group in the α-position has an even more profound effect on the binding affinity as can be seen from the titration curve of **4m** with α-ketobutyric acid. The binding of the guest in this case is best described by a 1:2 model with a K_1K_2 of $1.0(2) \times 10^6$ M^{-2}, which corresponds to an average binding constant of ca. 10^3 M^{-1} for each successive step (Figure S63, Supporting Information). It should also be noted that binding of the ketoacid is accompanied by a substantial change in the chemical shift of the amide proton, thus excluding the possibility that the observed increase in binding is related only to the decrease in the pK_a value.

Binding of α-ketoglutaric acid shows even more significant changes in the amide chemical shift (Figure S56, Supporting Information) and the stoichiometry of the acid; the **4m**:α-ketoglutaric acid complex was confirmed to be 1:1 by a Job's plot (Figure S64, Supporting Information). Unfortunately, due to the decrease of the chemical shift of the amide proton after addition of 1 equiv of the guest (presumably related to protonation effects), no good fit of the binding curve could be obtained, but the association constant in this case is estimated to be at least 10^3 M^{-1}, which is consistent with the results obtained for α-ketobutyric acid, and shows substantial selectivity of **4m** toward substrates with a keto group capable of forming additional hydrogen bonds with the host molecule.

Conclusion

We have designed and synthesized five macrocyclic compounds that contain amide and amino groups and have studied the effects of the ring size on topicity of anion binding as well as the influence of secondary amino groups on anion recognition by 2,6-bis(carbamoyl)fragments. Secondary amino groups can be protonated and can serve as additional hydrogen bond donors, which results in high selectivity of hosts to the size and shape of the carboxylic acids and inorganic oxoanions as guests. These effects are less important for the fluoride anion.

We have applied a novel approach to study topicity of anion binding in macrocyclic structures by comparing properties of macrocycles from [1 + 1] versus [2 + 2] condensations, thereby examining the effect of cavities of different sizes. We have established that the minimum ring size of the 2,6-bis(carbamoyl)pyridine-containing macrocycle to bind fluoride is 15. Complexation of fluoride has a significant water dependence,

suggesting competitive binding of water and fluoride. Preliminary studies suggest a 2:1 binding mode of F^- to **4**. We have obtained indirect evidence of ditopic complexation of dicarboxylate ions in solution; the newly synthesized macrocycle **4** possesses much higher affinity to dicarboxylates compared to monocarboxylates.

Macrocycle **4** exhibits a substantial length selectivity for binding of dicarboxylic acid/dicarboxylates, despite their very similar pK_a values. The crystal structure of an adduct of **4** with *p*-nitrobenzoic acid suggests the importance of the amino group adjacent to the 2,6-bis(carbamoyl)pyridine moiety for effiecient carboxylic acid binding.

Methylation of secondary amino groups (macrocycle **4m**) decreases the number of hydrogen bond donors compared to nonmethylated **4** and leads to increase of steric bulk inside the macrocyclic cavity. This results in generally lower binding constants for both inorganic and organic anions with **4m**. Despite that, **4m** exhibits high selectivity toward α-ketocarboxylic acids.

Experimental Section

General. ^{1}H and ^{13}C NMR spectra were referenced to the residual solvent peak (^{1}H $\delta(CHCl_3) = 7.27$ ppm, $\delta((CHD_2S(O)CH_3) = 2.50$ ppm) or to the solvent peak (^{13}C $\delta(CDCl_3) = 77.23$ ppm, $\delta((CD_3)_2SO) = 39.51$ ppm). ^{19}F NMR spectra were referenced to an external standard ($\delta(CF_3CO_2H)$ in $(CD_3)_2SO$ was assumed to be −76.55 ppm). Anion binding to macrocyclic ligands was studied by ^{1}H NMR titrations. A solution of macrocycle (0.500 mL, 10 mM) in DMSO-d_6 was placed in an NMR tube, aliquots of solution of a titrant (100 mM) were added, and the spectra were recorded. Binding curves were fit by using the program Wineqnmr.[32] The quality of fit was estimated by using the "merit-function" shown in eq 11 where W_i is the weight attributed to observation i (normally data points were assigned equal weights):

$$R = 100\left(\frac{\sum W_i(\delta_{obs} - \delta_{calc})^2}{\sum W_i(\delta_{obs})^2}\right)^{1/2} \quad (1)$$

Samples for Job's plots were prepared by first mixing a solution of the macrocycle (250 μL, 10 mM) with a solution (250 μL, 10 mM) of the guest. The exact concentrations of the guest and host macrocycle solutions were determined from this experiment and then used for the calculations of the volumes of the host and the guest solutions, so that the total number of moles was constant throughout the series.

X-ray Crystallographic Study. Data were collected with a Bruker SMART CCD (charge coupled device) based diffractometer. A suitable crystal was chosen and mounted on a glass fiber with Paratone-N oil. Data were measured by using omega scans of 0.3° per frame for 30 s, such that a hemisphere was collected. A total of 1650 frames for **2b**, **4·2MeOH**, **4m·2MeOH**, **4·2(CH$_2$)$_3$(CO$_2$H)$_2$·9H$_2$O**, **4·2DMSO**, and **4·4(4-NO$_2$C$_6$H$_4$CO$_2$H)**, and a total of 1271 frames for **2a** were collected with a maximum resolution of 0.75 Å. The first 50 frames were recollected at the end of data collection to monitor for decay. Cell parameters were retrieved by using SMART[49] software and refined with SAINT on all observed reflections. Data reduction was performed with the SAINT software,[50] which corrects for Lp.

The structures were solved by the direct method by using the SHELXS-97[51] program and refined by least-squares method on F,[2] SHELXL-97,[52] incorporated in SHELXTL V5.10.[53] All non-hydrogen atoms are refined anisotropically. The structures of **4·2MeOH** and **4·2DMSO** were solved in the space group $P\bar{1}$ (no. 2) for by analysis of systematic absences. Hydrogen atoms were calculated by geometrical methods and refined as a riding model. In all cases the compound lies on an inversion center.

The structure of **1·HClO$_4$** was solved in the space group $Pna2_1$ (no. 33) by analysis of systematic absences. All non-hydrogen atoms are refined anisotropically. Hydrogen atoms are refined isotropically. Hydrogen atoms at N4 and N5 are refined at 75% occupancy.

The structure of **2b** was solved in the space group $P2_1/c$ (no. 15) by analysis of systematic absences. Hydrogen atoms were located on a Fourier difference map and refined isotropically.

The structure of **2a** was solved in the space group *Pcab* (no. 61) by analysis of systematic absences. Hydrogen atoms were calculated by geometrical methods and refined as a riding model.

The structure of **4m·2MeOH** was solved in the space group $P2_1/n$ (no. 14) by analysis of systematic absences. Hydrogen atoms were calculated by geometrical methods and refined as a riding model.

The structure of **4·2(CH$_2$)$_3$(CO$_2$H)$_2$·9H$_2$O** solved in the space group $P\bar{1}$ (no. 2). Carbon-bound hydrogen atoms were calculated by geometrical methods and refined as a riding model. Nitrogen-bound hydrogen atoms were located on a Fourier difference map and refined isotropically. Hydrogen atoms bonded to the amine nitrogens were refined at 50% occupancy. Hydrogen atoms in the water molecules were located on a Fourier difference map and refined isotropically with the O−H bond length restrained to 0.95 Å.

The structure of **4·4(4-NO$_2$C$_6$H$_4$CO$_2$H)** was solved in the space group $P\bar{1}$ (no. 2). Carbon-bound hydrogen atoms were calculated by geometrical methods and refined as a riding model. Nitrogen-bound hydrogen atoms were located on a Fourier difference map and refined isotropically.

All drawings are done at 50% ellipsoids. The crystals used for the diffraction study showed no decomposition during data collection.

CCDC contains the supplementary crystallographic data for this paper: **1·HClO$_4$** (623337), **2a** (620614), **2b** (620617), **4·2MeOH** (620619), **4·2DMSO** (620620), **4m·2MeOH** (623339), **4·2(CH$_2$)$_3$(CO$_2$H)$_2$·9H$_2$O** (623340), and **4·4(4-NO$_2$(C$_6$H)$_4$CO$_2$H)** (623338). These data can be obtained free of charge via www.ccdc.cam.ac.uk/data_request/cif, or by emailing data_request@ccdc.cam.ac.uk, or by contacting The Cambridge Crystallographic Data Centre, 12, Union Road, Cambridge CB2 1EZ, UK; fax: +44 1223 336033.

Materials. All materials used were ACS reagent grade or better and were used without additional purification. 2,6-Pyridinedicarboxylic acid dimethyl ester,[54] $H_2PyDioneN_5$ (**1**),[30] and **2b**[31] were synthesized according to previously reported procedures. **2a**, **3**, and **4** were prepared according to the procedures published in the preliminary report.[6] Tetrabutylammonium salts—acetate, fluoride (1 M solution in THF), hydrogen sulfate, iodide, perchlorate, and dihydrogen phosphate (1 M aqueous solution)—were used as received. The tetraethylammonium salts were synthesized from tetraethylammonium hydroxide and the corresponding acid, the salts were dried in vacuo by azeotropic distillation of water with toluene. Importantly, the drying temperature should not exceed 20 °C to minimize decomposition of the salt.

Syntheses. Macrocycle 4m: 4 (554 mg, 1.0 mmol) was dissolved in a mixture of formic acid (4.21 g of 88% solution) and formaldehyde (3.24 g of 37% aqueous solution). The resulting reaction mixture was refluxed overnight and the crude product was purified by chromatography on neutral alumina (25 mm × 8 cm, 300 mL of $CHCl_3$/MeOH (10:1) eluent). The solvent from the

(49) *SMART V 5.050 (NT)*, Software for the CCD Detector System; Bruker Analytical X-ray Systems: Madison, WI, 1998.
(50) *SAINT V 5.01 (NT)*, Software for the CCD Detector System; Bruker Analytical X-ray Systems: Madison, WI, 1998.
(51) Sheldrick, G. M. *SHELXS-90*, Program for the Solution of Crystal Structure; University of Göttingen: Göttingen, Germany, 1990.
(52) Sheldrick, G. M. *SHELXL-97*, Program for the Refinement of Crystal Structure; University of Göttingen: Göttingen, Germany, 1997.
(53) *SHELXTL 5.10*, PC-Version, Program library for Structure Solution and Molecular Graphics; Bruker Analytical X-ray Systems: Madison, WI, 1998.
(54) Dierck, I.; Herman, G. G.; Goeminne, A. M.; Van der Kelen, G. P. *Bull. Soc. Chim. Belg.* **1993**, *102*, 63–66.

collected fractions was removed in vacuo to produce white solid **4m**. The product is obtained in solid form and is additionally purified by recrystallization from MeOH. Yield after recrystallization is 210 mg (34%).

^{1}H NMR (300 MHz, $CDCl_3$) δ 8.91 (t, ^3J(H,H) = 5.5 Hz, 2H, −C(O)N*H*−), 8.32 (d., ^3J(H,H) = 7.8 Hz, 2H, β-H), 8.03 (t, ^3J(H,H) = 7.8 Hz, 1H, γ-H), 3.45 (q, ^3J(H,H) = 5.7 Hz obs, 4H, −C(O)NHCH_2−), 2.48 (t, ^3J(H,H) = 5.4 Hz, 4H, −C(O)-NHCH$_2$CH_2−), 2.42 (s, 4H, −CH$_2$NHCH_2CH_2NHCH$_2$−), 1.92 (s, 6H, NCH_3). ^{13}C NMR (75 MHz, $CDCl_3$) δ 164.4, 150.2, 139.0, 125.1, 55.7, 54.7, 42.7, 37.3. HRMS (ESI TOF), *m*/*z* 611.3772 (expected for [M + H$^+$] 611.3776, error –0.7 ppm), 633.3613 (expected for [M + Na$^+$] 611.3596, error 2.7 ppm). ^{1}H NMR (300 MHz, DMSO-d_6) δ 9.19 (t, ^3J(H,H) = 6.0 Hz, 2H, −C(O)N*H*−), 8.22–8.12 (m, 3H, β,γ-H of the pyridine ring), 3.42 (q, ^3J(H,H) = 6.1 Hz obs, 4H, −C(O)NHCH_2−), 2.52 (t, ^3J(H,H) = 6.3 Hz, 4H, −C(O)NHCH$_2$CH_2−), 2.46 (s, 4H, −CH$_2$NHCH_2CH_2NHCH$_2$−), 2.19 (s, 6H, NCH_3).

Acknowledgment. This research was supported by the DOE (DE-FG02-06ER15799). The NMR and the mass spectroscopy facilities in the Chemistry Department at Tufts University were supported by NSF grants CHE-9723772 and CHE-0320783. The CCD based X-ray diffractometers at Tufts University and at Harvard University were purchased through Air Force DURIP Grant F49620-01-1-0242 and through NIH grant 1S10RR11937-01, respectively. The authors thank Scott Shandler for his help in preparing the cover art.

Supporting Information Available: ORTEP plots, NMR spectra for **4m**, titration curves, and Job's plots, a table summarizing crystallographic data, and crystallographic data in CIF format. This material is available free of charge via the Internet at http://pubs.acs.org.

JO800128R